Low-Momentum End of the Spectra of Heavy Primary Cosmic Rays*†

R. A. Ellis, Jr.,‡ M. B. Gottlieb, and J. A. Van Allen
Department of Physics, State University of Iowa, Iowa City, Iowa

(Received March 8, 1954)

Measurements of the intensity of heavy primary cosmic-ray nuclei have been made above the atmosphere by means of the new Iowa balloon-launched rocket ("rockoon") technique at geomagnetic latitudes $\lambda=56°$, 76°, and 86°. The measuring instrument was a thin-walled, pulse-ionization chamber of 15-cm diameter. The observed data, in conjunction with geomagnetic theory, demonstrate a complete or nearly complete absence of primary heavy nuclei of $Z\geq 6$ having a magnetic rigidity less than 1.5×10^9 volts ($p/mc<0.8$), the result being the most significant for the C, N, O group. It is noted that this spectral cutoff occurs at closely the same magnetic rigidity, and distinctly not at the same velocity, as the previously reported cutoff in the spectra of primary protons and α particles.

I. INTRODUCTION

RECENT investigations[1–5] of the dependence of cosmic-ray intensity at high altitude upon geomagnetic latitude make it abundantly clear that there occurs a marked and rapid change in form of the integral number-magnetic rigidity spectrum of the primary radiation at a rigidity R (momentum-to-charge ratio pc/Ze) of about 1.5×10^9 volts. In particular,[4] there appears to be a complete or nearly complete absence of primary protons in the magnetic rigidity range 1.2×10^9 volts to 0.18×10^9 volts (kinetic energy range 590 Mev to 18 Mev), and of primary alpha particles in the magnetic rigidity range 1.2×10^9 volts to 0.37×10^9 volts (kinetic energy range 700 Mev to 72 Mev).

But because of the low relative abundance of heavy primary nuclei (atomic number $Z>2$) these results do not make possible any significant conclusion as to their presence or absence in the low-momentum portion of their spectra.

Substantial progress has been made in the determination of the spectra of heavy primaries at rigidities greater than 1.5×10^9 volts, principally by means of balloon-borne photographic emulsions. But the available data approaching the low-rigidity end of the spectrum are in substantial disagreement. Thus, the Minnesota group[6] reports a steepening of the integral number spectrum of nuclei of $Z\geq 10$ toward low energies, whereas the Rochester group reports a flattening.[7] Indeed, the definitive investigation of the low-rigidity portion of the spectra of heavy particles is, at present, impractical by balloon methods due to the altitude limitation of balloon flights. Most of the balloon data have been obtained at residual atmospheric depths of about 15 g/cm². Even at depths as small as 10 g/cm², investigation of this matter is prevented simply by the short ionization range of those particles whose presence, or absence, it is desired to determine. The quantitative nature of this limitation is exhibited in Fig. 1.

The question of the presence or absence of low-momentum (or low-rigidity) heavy primaries is, however, a matter of keen interest in connection with the astrophysical origin of the cosmic radiation and with its propagation to the earth. Any proposed mechanism of origin, any postulated amount of interstellar material traversed, and any postulated system of magnetic fields must eventually be tested against observed data bearing on this question. It is evident from Fig. 1 that high-altitude rocket techniques are uniquely suited to this observational undertaking. To fully exploit such techniques, it is further necessary to minimize the wall thickness of the detecting apparatus and to make the flights at sufficiently high latitude as to be free of geomagnetic limitations.

The new Iowa balloon-launched rocket ("rockoon") scheme[4] makes it possible to fly 30 pounds of apparatus to some 100-km altitude at a vehicle cost less than that of a large Skyhook balloon flight.

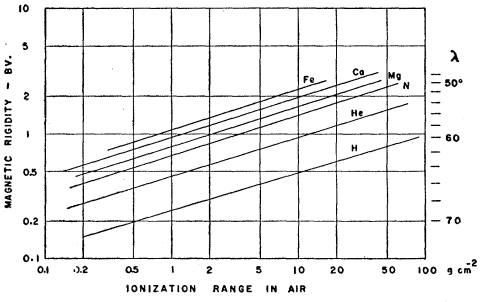

FIG. 1. Ionization range in air of representative nuclei as a function of magnetic rigidity. Curves derived from pp. 40–41 of reference 14 on assumption of complete stripping. Scale of ordinates on the right gives geomagnetic latitude at which vertical geomagnetic cutoff equals magnetic rigidity on the left.

* Based on doctoral dissertation of R. A. Ellis, Jr., February, 1954 (unpublished).

† Assisted by joint program of the U. S. Office of Naval Research, the U. S. Atomic Energy Commission, and the Navy Bureau of Aeronautics; and by the Research Corporation.

‡ Present address: Department of Physics, Tennessee Agricultural and Industrial State University, Nashville, Tennessee.

[1] J. A. Van Allen and S. F. Singer, Phys. Rev. **78**, 819 (1950); **80**, 116 (1950).
[2] J. A. Van Allen and S. F. Singer, Nature **170**, 62 (1952).
[3] Neher, Peterson, and Stern, Phys. Rev. **90**, 655 (1953).
[4] J. A. Van Allen, Nuovo cimento **10**, 630 (1953).
[5] Meredith, Van Allen, and Gottlieb, Phys. Rev. (to be published).
[6] Freier, Anderson, Naugle, and Ney, Phys. Rev. **84**, 322 (1951).
[7] Kaplon, Peters, Reynolds, and Ritson, Phys. Rev. **85**, 295 (1952).

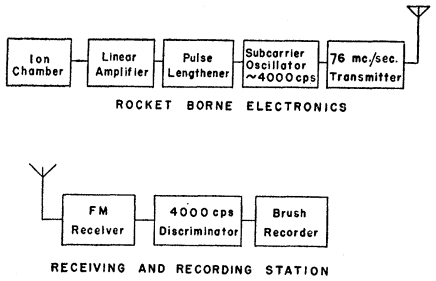

FIG. 2. Block diagram of circuitry and radio telemetering system.

It has been shown[8–10] that thin-walled pulse ionization chambers are effective detectors of heavy primaries and that it is possible to construct such chambers and associated electronic circuits which can be installed in rockets and adapted to conventional telemetering systems. The burst size distributions obtained during the time that thin-walled ionization chambers are effectively above the atmosphere are, primarily, the result of direct traversals of heavy primaries. From the analysis of such burst size distributions obtained in the geomagnetic latitude range from 56° to 90°, it is possible to determine the form of the low-momentum end of the spectra of heavy primaries over the momentum range from the vertical geomagnetic cutoff at about 56° to the cutoff due to the finite wall thickness of the apparatus.

The present report is based on data obtained in four successful rocket flights and one balloon flight (in which the rocket failed to fire) on a shipboard expedition to northerly latitudes during the summer of 1953.

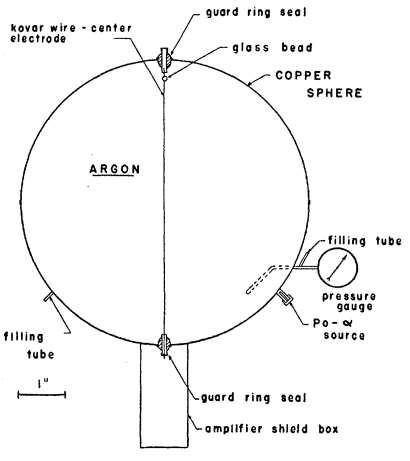

FIG. 3. Thin-walled pulse-ionization chamber. The chamber was supported by a "bowl" of Styrofoam in the extreme forward end of the nose shell of the rocket. Surrounding material was minimized.

[8] T. Coor, Jr., Phys. Rev. **82**, 478 (1951) and doctoral dissertation, Princeton University, August, 1948 (unpublished).
[9] J. A. Van Allen, Phys. Rev. **84**, 791 (1951).
[10] M. Pomerantz and G. W. McClure, Phys. Rev. **86**, 536 (1952).

II. DESCRIPTION OF APPARATUS

A block diagram of the system used in this experiment is shown in Fig. 2. The ionization chamber and the associated circuitry were mounted in the nose shell of a Deacon rocket which was carried to an altitude of about 60 000 feet by a General Mills model 551-A plastic balloon and fired by either a pressure or time switch.[11] The data were transmitted to the ship by an FM-FM telemetering system. The nose shells were aluminum and had an average wall thickness of 0.050 inch.

The ionization chambers were fabricated from copper hemispheres, six inches in diameter and 0.010-inch average wall thickness. The collecting electrode was a 0.025-inch Kovar wire which was soldered into a guard ring system made from Stupakoff seals. Figure 3 shows the details of the ionization chamber.

A fairly thin polonium alpha source was permanently mounted in each chamber to provide an absolute system calibration for burst size. These sources were prepared by a method described by Hulsizer,[12] and were mounted $2\frac{1}{4}$ mm outside the inner surface of the chamber wall such that a $\frac{1}{16}$-inch diameter hole in the wall served to collimate the beam of alpha particles. The sources chosen produced from twenty to sixty pulses per minute at the time of flight. Figure 4 is an integral number bias curve obtained from a typical chamber with an electronic pulse-height analyzer, and Fig. 5 is the same type of curve obtained from the same chamber over the complete telemetering system.

The program for filling the chambers was the following: the chambers were pumped on for twenty-four hours with a mechanical pump while they were maintained at a temperature of approximately 80°C by heat lamps; after cooling, 99.6 percent pure argon was admitted to the chambers to a pressure of about 15 psi and circulated over hot calcium (100°C) for twenty-four hours; the filling system was allowed to come to thermal equilibrium with the surroundings and the pressure was dropped to about 10 psi on a calibrated "standard" gauge just prior to sealing off the chambers with soft solder. The exact reading of the standard gauge was chosen in accordance with the ambient laboratory temperature and pressure to yield a sealed-off pressure of 1.50 atmospheres at 0°C, 760 mm of Hg. An inexpensive pressure gauge was left permanently connected to the chamber to indicate any subsequent leakage.

These chambers were operated as electron collection chambers with the center wire at high positive potential. The gas purity was considered adequate when identical integral number bias curves were obtained for the polonium alpha sources for sweeping voltages of 600 and 900 volts. Each of the chambers satisfied this criterion from the time of its initial filling until it was

[11] J. A. Van Allen and M. B. Gottlieb, Rev. Sci. Instr. (to be published).
[12] R. I. Hulsizer, dissertation, Massachusetts Institute of Technology, 1950 (unpublished).

flown about three months later. The chambers were flown with 900 volts sweeping voltage. The enclosing nose shells were sealed at sea level pressure to prevent any possibility of corona when the apparatus was at high altitudes. The counting rate of bursts larger than the bursts from the polonium source due to radioactive contamination was less than one burst per minute for each chamber.

The pulse amplifiers had a rise time of about 2 microseconds, a decay time of about 40 microseconds, and a voltage gain of about 2000. The gain of these amplifiers was not measurably different over the range 75 to 100 volts of the B^+ supply voltage.

The short-duration pulses from the amplifier were lengthened and given a characteristic shape for the purpose of satisfactory telemetering transmission and recording. The lengthened pulses had a width of about 15 milliseconds at half-height and their amplitude was accurately related, though not proportional, to the

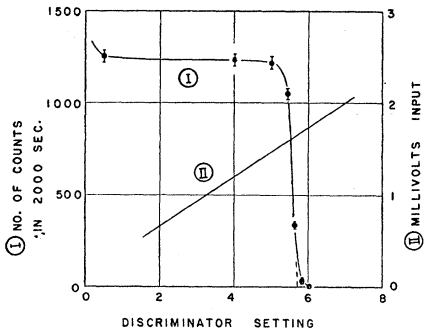

FIG. 4. Typical integral number bias curve (I) of bursts from Po—α particle source. Output of linear amplifier was fed to a commercial pulse-height analyzer. Ordinate scale of curve I to left. Ordinate scale of calibration curve (II) to right.

input pulse amplitude. There was no change in the performance of this circuit over a range of the supply voltage of 60 to 90 volts. Loss of counts due to finite pulse width was negligible at the maximum observed counting rate of about 2 counts/sec (due to cosmic-ray events plus calibrating Po—α's). The pulse lengthening circuit was modelled after one described by Elmore and Sands.[13]

Raytheon rugged subminiature tubes, such as the CK5678, were used throughout all circuits—with the exception of the telemetering transmitter, in which a 3A5 was used.

The subcarrier oscillator was a voltage-controlled frequency-modulated audio-oscillator. The nose shell and body of the rocket, which were insulated from each other, formed the arms of an asymmetrical dipole transmitting antenna.

A two-bay Yagi antenna, a Clarke Instrument Company FM telemetering receiver, an audio discriminator,

[13] W. C. Elmore and M. Sands, *Electronics* (McGraw-Hill Book Company, Inc., New York, 1949), p. 196.

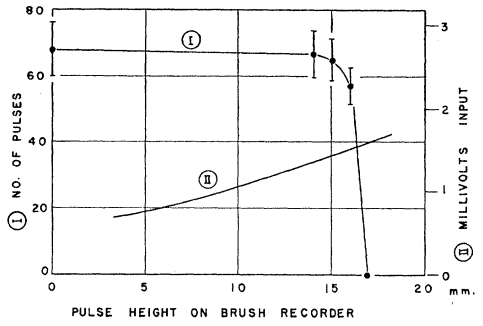

FIG. 5. Typical integral number bias curve (I) for Po—α source as obtained over complete telemetering system as shown in Fig. 2. Curve II is calibration curve. Scales of ordinates as in Fig. 4.

Model BL 905 Brush amplifier, and Model BL 202 Brush inking oscillograph comprised the receiving station. It was possible to record data without evidence of noise with a radio signal input to the receiver as low as 4 microvolts.

A meterological radiosonde was sent up with each flight to provide pressure-altitude *vs* time-data for the ascent to the firing altitude.

The entire instrumentation was turned on about a half-hour before release of the rockoon system from the ship. From then on it was in continuous operation during final preparations for release, during the balloon phase of the ascent and during the final free-rocket flight until eventual destructive impact with the sea.

The capacity of the batteries used was great enough to insure that the decline in voltages during the entire period of operation was slight enough to allow the application of the preflight calibration throughout, a period of not more than two and a half hours. In addition to this general provision, the built-in polonium alpha source provided an over-all system calibration throughout the balloon and rocket phases of the flight. The entire electronic system, including radio telemetering link and receiving station was also calibrated over its full range immediately before a flight by introducing step pulses of known size (from a battery and mercury switch) directly on the center wire of the ionization chamber and recording the output pulses on the Brush oscillograph in the telemetering receiving station. Figure 6 is a plot of the results of such a calibration.

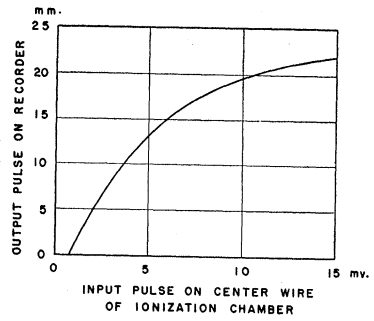

FIG. 6. Over-all calibration of complete system of Fig. 4.

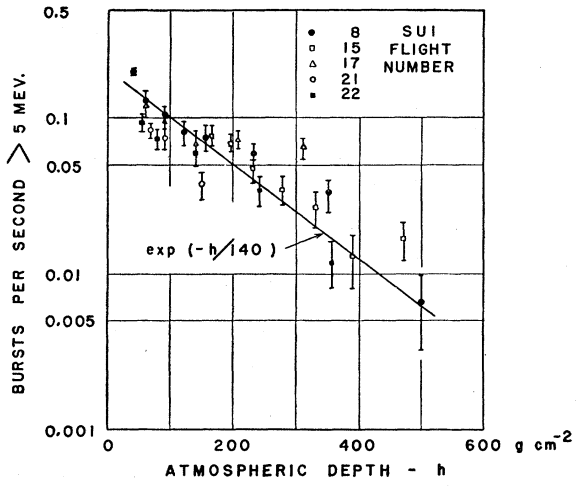

FIG. 7. Counting rates of bursts larger than 5 Mev as observed during balloon-ascent phase of Flights 8, 15, 17, 21, and 22. For comparison a curve of the form $\exp(-h/140)$ has been drawn among the observed points.

These calibration curves were reproducible to within 3 percent.

The conversion of the experimental data to an absolute scale was achieved by combining the system calibration and the pulse-height distribution due to the polonium alpha source (Figs. 4 and 5). The number of millivolts equivalent to a polonium alpha burst was taken to be the number of millivolts required to produce a pulse the size of the extrapolated integral pulse height for the polonium alpha distribution. The number of millivolts equivalent to one polonium alpha lay within a 0.1-millivolt range for each chamber for several determinations during the period between assembly and launching. This correspondence between pulse height and energy lost in the chamber is strictly true only for ion pairs produced near the wall because of the dependence of pulse-height on position of the ion pairs in electron collection chambers.[14] The dependence of pulse height on position was measured for these chambers by moving a probe with a polonium-alpha source on the end to various positions in the chamber and observing the pulses from the chamber's amplifier on a fast oscilloscope. No change in pulse height to within 5 percent was observed as a function of position.

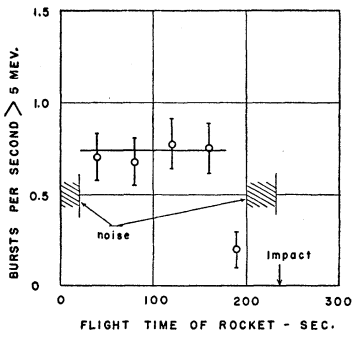

FIG. 8. Counting rate of bursts greater than 5 Mev during rocket phase of Flight 15.

Since the polonium alpha source was $2\frac{1}{4}$ mm outside the inner wall of the ionization chamber, the energy loss in the sensitive volume of the chamber must be calculated from range-energy data for alpha particles.[15] From the empirical range-energy relationship and the fact that the range of a polonium alpha particle in argon at 760 mm Hg pressure and 15°C is 41.4 mm, the energy lost in the ionization chamber by a polonium alpha particle from the source was found to be 5.0 Mev.

The basic amplifier noise level corresponded to about 0.15 Mev (Fig. 4). But due to the threshold characteristic of the pulse lengthener using subminiature tubes, the minimum measurable burst size was about 3.5 Mev (Fig. 6). This minimum could have been reduced but it was felt to be suitable for this application.

In argon, a minimum ionizing singly charged particle loses energy at the average rate of 1.49 Mev/(g cm^{-2}).

TABLE I. General flight data.

Flight number	8	15	17	21	22
Position of release of balloon (geographical)	42°26′N 70°22′W	64°20′N 59°06′W	74°23′N 71°56′W	44°50′N 57°13′W	44°45′N 57°10′W
Date (1953)	July 18	Aug. 6	Aug. 9	Sept. 3	Sept. 3
Time of launching of rockoon (Greenwich standard time)	2227	1507	0554	0950	1151
Estimated geomagnetic latitude of rocket flight (centered dipole)	53°	76°	86°	56°	56°
Estimated altitude of firing of rocket (feet above sea level)	Did not fire	45 000	68 000	67 000	67 000
Estimated summit altitude (feet above sea level)	73 000	225 000	325 000	300 000	340 000
Duration of plateau (seconds)	···	160	200	163	220

For a diametrical traversal of one of these chambers, such a particle loses 0.06 Mev. For the traversal of the same thickness of matter, the energy lost by a minimum ionizing particle of charge Ze is Z^2 times that lost by a singly-charged minimum-ionizing particle. Note that the simultaneous diametrical traversal of 86 minimum-ionizing singly-charged particles is required to produce a burst of 5 Mev.

Further experimental and circuitry details are available in the doctoral dissertation (1954) of R. A. Ellis, Jr. on file at the State University of Iowa, and in reference 11.

III. RESULTS

Table I gives the date, time of launching, latitude, firing altitude, estimated peak altitude, and time duration of high-altitude plateau of each flight.

[14] B. Rossi, *High Energy Particles* (Prentice-Hall, Inc., New York, 1952).

[15] J. O. Hirschfelder and J. L. Magee, Phys. Rev. **73**, 207 (1948).

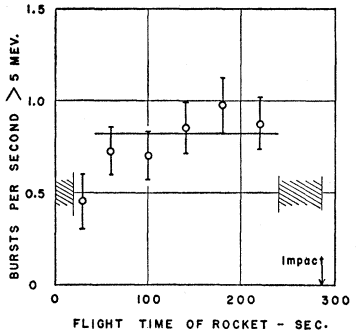

FIG. 9. Counting rate of bursts greater than 5 Mev during rocket phase of Flight 17.

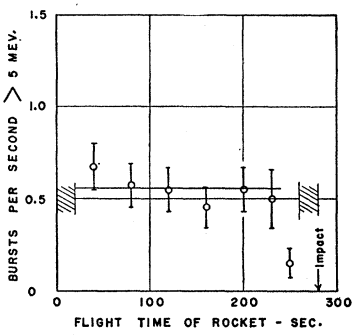

FIG. 11. Counting rate of bursts greater than 5 Mev during rocket phase of Flight 22.

The counting rate of cosmic-ray bursts larger than 5 Mev as a function of altitude for the balloon portion of all of the flights is shown in Fig. 7. For comparison, a curve of the form $\exp(-h/140)$ has been drawn among the observed points;[14] h is the atmospheric depth in g/cm^2.

An interesting check is that the observed counting rate of bursts larger than 5 Mev in these 6-inch diameter chambers was very closely equal to one-fourth the counting rate of bursts larger than 5.1 Mev observed by Coor[8] at 52° using spherical ionization chambers of 12-inch diameter—the ratio being independent of altitude up to 40 g/cm^2 (the highest balloon flight data of the present investigation).

The raw burst size distributions obtained below 30 000 feet (300 g/cm^2) were almost entirely due to calibrating Po—α's. Hence for each flight, the corresponding distribution of bursts below 30 000 feet, normalized to the appropriate time interval, was subtracted from the total observed high-altitude data to obtain the net distribution of cosmic-ray bursts.

Ideally, the counting rate of bursts of all sizes as a function of time during the rocket portion of the flight may be expected to show an initial rapid increase; to level off at a constant value, which is referred to as the "plateau" counting rate; and finally to decrease rapidly as the ionization chamber is carried back down through the atmosphere. The duration of the constant-counting-rate period should be the time during which the sum of the atmospheric path and the apparatus wall thickness has a negligible effect on the primary radiation. The actual flight data show the expected plateaus but only an indication of the increase and decrease in the counting rate expected at the beginning and end, respectively, because of the loss of satisfactory signal due to microphonics. These microphonics, which could be produced in the laboratory by tapping the ionization chamber and/or the amplifier, are presumed to be excited by vibration of the rocket during the noisy burning period of the motor and by aerodynamic flutter of tail fins, etc., during passage through the denser atmosphere. They are commonly observed in rocket flights of high-gain amplifiers.

The flight periods above 40 km for which burst data are given appeared to be entirely free of microphonics. In one case only there were a few seconds of lost time due to weakening of the radio signal. This effect in the received signal is altogether different than that due to microphonics and is confirmed by readings of the input signal to the receiver.

Figures 8, 9, 10, and 11 show the observed counting rate curves for bursts larger than 5 Mev for the four successful rocket flights, from the time of firing to the time of impact.

The data from the plateaus of the rocket flights are presented in Fig. 12 as integral burst size distributions. The flight data are consolidated in Table II together with data obtained from Flight 8 for a twenty minute period during which the pressure-altitude data showed that the balloon and the suspended rocket remained at an altitude of 40 plus or minus 5 g/cm^2. Figure 13, which is a plot of the raw and corrected distributions from the plateau of Flight 21, shows clearly the manner in which the polonium alpha source contributed to the experimental distributions. The best flight evidence that

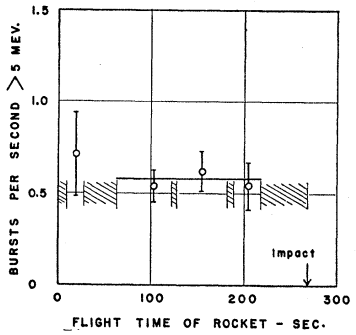

FIG. 10. Counting rate of bursts greater than 5 Mev during rocket phase of Flight 21.

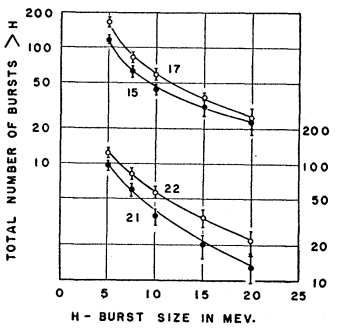

FIG. 12. Integral burst size distributions for high altitude plateau periods of Flights 15, 17, 21, and 22. Time duration of plateau period is different for each. Ordinate scale for Flights 15 and 17 on left, for Flights 21 and 22 on the right.

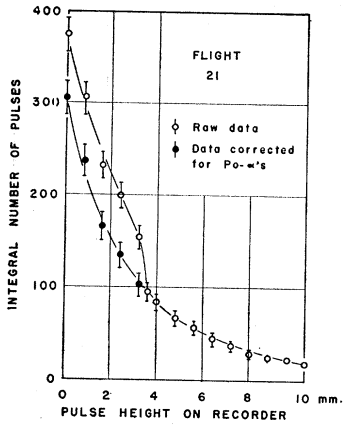

FIG. 13. Raw pulse-height distribution for high-altitude plateau period of Flight 21, and distribution after subtraction of pulses due to the calibrating Po—α source.

the different chambers could be considered identical in the interpretation of the data is found in the burst size distribution from Flights 21 and 22 which were made within three hours of each other at nearly the same location. The data from Flights 21 and 22 are plotted in Fig. 14. From Figs. 7 and 14 it is seen that the counting rates from these two chambers are in good agreement. In Table II the data from Flights 21 and 22 are combined.

IV. BASIS FOR INTERPRETATION

A. Causes of Bursts of Ionization

Coor[8] has pointed out that the only significant causes of bursts in an ionization chamber at high altitudes are: (a) traversals of single particles through the chamber without nuclear interactions in the chamber or its surroundings and (b) the passage through the chamber of the charged products of nuclear interactions (stars) produced in the chamber walls, the gas of the chamber, and the immediate surroundings.

B. Contributions of Stars to Plateau Data

An estimate of the contribution of nuclear interactions, due to all causes, in the walls and surroundings of the chambers while above the atmosphere can be based on the burst distribution obtained in Flight 8 at 73 000 ft (40 g cm^{-2}) (Table II), and the altitude dependence of stars in photographic emulsions reported by Lord.[16] Such an estimate is considered sufficiently applicable to all of the flights, even though Flight 8 was made at $\lambda = 53°$ (λ denotes geomagnetic latitude in the centered-dipole approximation to the earth's magnetic field), because the total omnidirectional intensity above the atmosphere[4,5] increases by only about 25 percent between $\lambda = 53°$ and $\lambda = 89°$.

It appears that the counting rate of all bursts at 40 g cm^{-2} can be safely adopted as an *upper limit* to the counting rate above the atmosphere of bursts due to nuclear interactions because the observed maximum in altitude-dependence of star production occurs at about this depth[16] and because the omnidirectional intensity of neutrons (the major producers of stars within the atmosphere) has been shown to fall off near the top of the atmosphere.[17] Accordingly, by reference to Table II, it is seen that stars represent a contribution of less than 36 percent to the observed rate of plateau bursts larger than 5 Mev, less than 18 percent to bursts larger than 10 Mev, and a negligible contribution to bursts larger than 20 Mev. This conclusion is in agreement with Coor[8] and Van Allen,[9] who showed that the distribution of bursts due to nuclear interactions had relatively more small bursts than the distribution due to traversals of heavy primaries. A fuller discussion of this matter is given by Whyte[18] and by Pomerantz and McClure.[10]

Ionization bursts larger than 5 Mev from nuclear interactions are visualized as being due almost entirely to "black prongs" emerging from the inner skin of the ionization chamber wall and to those originating in the filling gas. Since the coincident, diametrical traversal of some 86 minimum ionizing singly charged particles is required to dissipate 5 Mev in the chamber, no significant fraction of the observed bursts can be due to "gray" and "minimum" tracks. The range of most black prongs does not exceed 0.3 g cm^{-2}; hence it is probably not feasible to substantially reduce the contribution of stars by further reduction of the wall thickness of the chamber.

An estimate of the contributions of stars from first principles has been attempted. Such an estimate serves to check the general reasonableness of the above conclusions but is not of sufficient reliability to add significantly to the preceding discussion.

C. Unlikelihood of Contributions to Plateau Burst Data by Particles of $Z \leq 2$

(a) The geometrical factor of a spherical chamber of radius r is $2\pi^2 r^2$ cm^2 steradian in a hemispherical flux field. For the chambers used, $r = 7.5$ cm and the geometrical factor had the value 1110 cm^2 steradian. Thus,

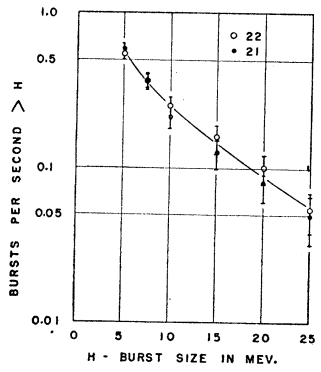

FIG. 14. Comparison of integral rate of bursts of size greater than H as a function of H for plateau period of Flights 21 and 22.

[16] J. J. Lord, Phys. Rev. **81**, 901 (1951).

[17] L. C. L. Yuan, Phys. Rev. **81**, 175 (1951).

[18] G. N. Whyte, Phys. Rev. **82**, 204 (1951).

above the atmosphere at the most northerly latitude, about 520 charged particles of all types pass through the chamber per second. The characteristics of the electron-collection chambers and the associated amplifier (Sec. II) were such that rate of "pileup" of accidentally coincident pulses to a detectable size was negligible by many orders of magnitude.

(b) The maximum expected energy which a proton can dissipate in the gas of the chamber by ionization is about 4 Mev if it makes a diametrical traversal and if it has precisely the optimum initial energy. Hence it is very unlikely that slow protons contribute to observed bursts of larger than 5 Mev. Likewise, single electrons cannot contribute.

(c) Slow α particles within a narrow energy range can, of course, contribute observable bursts of ionization, the maximum possible being about 14 Mev. The initial kinetic energy of an α particle upon its entrance into the chamber must lie between 5 Mev and 90 Mev in order that the expected ionization along a diametrical traversal exceed 5 Mev. The air range of a 90-Mev α particle is about 0.6 g cm^{-2} and its magnetic rigidity is 0.4×10^9 volts. Any such particles in the general nucleon cascade within the atmosphere are already included in the discussion of stars in Sec. IV-**B** above. *Primary* α particles of such a magnetic rigidity as would arrive at the apparatus above 50 km in the energy range 5–90 Mev are geomagnetically excluded south of $\lambda=65°$, and hence could not have contributed to the observations of Flights 21 and 22. And if, at the more northerly latitudes of Flights 15 and 17, there had been a sufficient intensity of such primary α particles, as a "slice" from a continuous spectrum, to contribute significantly to the observations, then there should have been a corresponding altitude dependence of the counting rate of bursts in the altitude range from 50 to 100 km. No such altitude dependence can be discerned in Figs. 8 and 9.

Hence, it is believed quite unlikely that primary α particles contribute to any observable extent to the observed rate of bursts of size greater than 5 Mev.

D. Interpretation of Observed Bursts as Due to Primary Particles of $Z>2$

Thus, by elimination, the interpretation of the plateau data in Flights 15, 17, 21, and 22 has been reduced to consideration of primary nuclei having Z greater than 2, and finally for *a posteriori* reasons to be mentioned later of nuclei having $Z\geq6$. No explicit subtraction of burst rate due to stars has been made due to uncertainty as to its exact magnitude; but in accordance with the discussion of Sec. IV-**B** it is thought that the star contribution does not exceed some 35 percent of the rate of bursts larger than 5 Mev and is probably lost in the statistical uncertainty of the rates of bursts larger than 10 and 20 Mev.

TABLE II. The observed burst size distributions. (From the high-altitude plateau portions of Flights 15, 17, 21, 22 and from a 20-minute period during which the apparatus of Flight 8 floated at 40 g cm^{-2}.)

Burst size, H (Mev)	Bursts/second greater than H (with statistical standard deviations) Flight 8 (40 g/cm^2)	Flight 15	Flight 17	Flights 21 and 22
5	0.203±0.015	0.738±0.081	0.850±0.065	0.566±0.038
7.5	0.112±0.011	0.408±0.051	0.425±0.046	0.368±0.031
10	0.044±0.006	0.293±0.043	0.285±0.038	0.238±0.025
15	0.015±0.004	0.204±0.036	0.185±0.030	0.144±0.019
20	···	0.159±0.032	0.115±0.024	0.091±0.015

E. Attenuation of the Intensity of Heavy Nuclei Before They Reach the Chamber

A detailed calculation shows that an average primary traversed 1.2 g cm^{-2} of matter (mostly copper and aluminum) in the apparatus before reaching the sensitive volume of the ionization chamber. When the plateau data were obtained, the rockets were above 50 km during practically all of the time intervals. The effective path length traversed in the atmosphere by an average primary for the altitude range between 50 and 100 km, the maximum altitude reached, was taken to be 0.6 g cm^{-2} on the basis of the air mass *versus* zenith angle tables of Pressly.[19] The interaction mean free path for iron nuclei, $Z=26$ (the most unfavorable case), according to Bradt and Peters,[20] is about 35 g cm^{-2} in the materials around the chambers. This means that considerably less than one in ten primary iron nuclei and an even smaller fraction of primary nuclei of smaller Z made a disintegrating collision before reaching the chamber.

F. Geomagnetic Considerations

In the calculation of burst size distributions for comparison with the experimental distributions, explicit faith has been placed in the geomagnetic theory of Stoermer and of Lemaitre and Vallarta as worked out for the simplified representation of the earth's magnetic field as that of a centered magnetic dipole of moment 8.1×10^{25} gauss cm^3 with axis piercing the surface of the earth at 78.5° N and 69.0° W, and at 78.5° S and 111.0° E. The papers from which numerical data were taken were those of Alpher[21] for general data and those of Schremp[22] and Koenig[23] for shadow-cone data. The Koenig plots of percent solid angle accessible to particles of a given magnetic rigidity for various geomagnetic latitudes were particularly convenient for the present purpose.

G. Calculation of Expected Burst Size Distributions

The raw burst size distributions admit an immediate impression as to the general nature of the latitude de-

[19] E. C. Pressly, Phys. Rev. **89**, 654 (1953).
[20] H. L. Bradt and B. Peters, Phys. Rev. **77**, 54 (1950).
[21] R. A. Alpher, J. Geophys. Research **55**, 437 (1950).
[22] E. J. Schremp, Phys. Rev. **54**, 158 (1938).
[23] H. P. Koenig, Phys. Rev. **58**, 385 (1940).

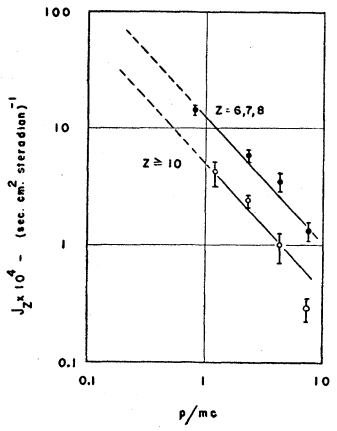

FIG. 15. Directional intensities of heavy nuclei from photographic emulsion work (references 7 and 24) as a function of minimum value of p/mc. See Sec. IV-G and Table III.

pendence of the intensity of heavy nuclei. But a much more refined interpretation is feasible and fruitful. The purpose of this section is to show how a calculated burst size distribution, for the chamber used, can be derived from fundamental data on the momentum spectra and absolute intensities of components of various Z. Comparison of the observed data with one or more families of calculated distributions can then be resorted to for the purpose of choosing the most nearly correct member of the family.

Spherical ionization chambers have the special virtue of presenting the same projected area to all directions. The burst size due to the traversal of a charged particle of a particular type depends on the path length in the gas of the chamber and on the average energy loss per unit distance due to ionization. Landau fluctuations and the dependence of the burst size on the position of formation of the ion pairs were neglected. The stopping power of the chamber gas was small enough so that the energy loss per unit distance could be considered constant over the path of a particle inside the chamber. Thus the burst size, due to the traversal of a particle which has a path length inside the chamber l and rate of ionization loss s per unit path length, is

$$H=kls. \tag{1}$$

A convenient set of dimensionless units is obtained by expressing l as the ratio of the actual path length to the diameter of the chamber and s as the ratio of the actual rate of ionization loss to the relativistic minimum rate. Then $k=1$ and H gives the burst size as the ratio of the actual burst size to that which would be produced when a minimum ionizing particle of the same type makes a diametrical traversal of the chamber. In these units, $H=ls$, and the calculated burst size applies to all types of particles, irrespective of Z.

The burst size distribution due to the traversal of particles through an ionization chamber can be calculated if the distributions of the particles with respect to s and l are known. For a sphere, the differential path length distribution $f(l)$ for a homogeneous flux of particles is independent of direction and is:

$$f(l)dl=2ldl, \quad 0\leq l\leq 1. \tag{2}$$

The distribution of particles with respect to s can be determined for any assumed distribution with respect to momentum p by using the Bethe-Bloch formula in the simplified form

$$s=1/\beta^2=1+(1/P^2), \tag{3}$$

wherein β is the ratio of particle velocity v to the velocity of light c; and P is the dimensionless ratio p/mc, with m as the rest mass of the particle. Relation (3) is of satisfactory accuracy in the range of present interest, namely $1\leq s\leq 60$.

In Fig. 15 are plotted the directional intensities of heavy nuclei derived from photographic emulsion data at various latitudes[7,24] as a function of the geomagnetic cut-off value of p/mc, P_c, in the vertical direction at the positions of the balloon flights in which they were obtained. (Numerically, $P\approx 0.52\times$ magnetic rigidity in units of 10^9 volts for all heavy nuclei.) The intensity of particles with $Z\geq 10$ at the most northerly latitude, is plotted at $p/mc=1.2$ (rather than at 0.8) because the residual atmosphere prevented particles of lesser value from reaching the emulsions. The data of Fig. 15 are well fitted, particularly for low values of p/mc, by an integral number spectrum of the form $KP^{-1.1}$, where K is a constant—a form identical to that proposed by Van Allen and Singer[1] for the total intensity spectrum over a similar range of P. Hence, in the range of P shown, the absolute directional intensity of particles with values of p/mc greater than P can be written

$$J(P)=KP^{-1.1}. \tag{4}$$

The corresponding differential number spectrum is

$$j(P)dP=(1.1KP^{-2.1})dP. \tag{5}$$

A differential distribution on s is obtained from Eqs. (3) and (5) as follows:

$$F(s)ds=j[P(s)]dP=j[P(s)](dP/ds)ds. \tag{6}$$

Thus,

$$F(s)=0.55K(s-1)^{-0.45}. \tag{7}$$

TABLE III. Adopted directional intensities.[a,b] (After Bradt, Peters, Kaplon *et al.*)

Nuclear charge Z	P	$Jz(P)\times 10^4$ sec^{-1} cm^{-2} sterad^{-1}	Kz in $Jz(P)=KzP^{-1.1}$
6	0.8	5	3.9
7	0.8	5	3.9
8	0.8	5	3.9
13	1.2	2.7	3.3
19	1.2	1	1.2
26	1.2	0.5	0.6

[a] See reference 7.
[b] See reference 24.

[24] Lal, Pal, Kaplon, and Peters, Phys. Rev. **86**, 569 (1952).

Over the domain of joint definition of $f(l)$ and $F(s)$, the rate that particles will traverse the chamber with s in ds and independently l in dl is proportional to

$$f(l)F(s)dlds. \tag{8}$$

Expression (8) is transformed to new variables $H=ls$ and s, with the result:

$$f(l)F(s)dlds=f(H/s)F(s)dHds\cdot\mathcal{J}\begin{pmatrix} l & s \\ H & s \end{pmatrix}, \tag{9}$$

wherein $\mathcal{J}(\ \ )$ is the Jacobian of the transformation. The right hand side of Eq. (9) is proportional to the rate of occurrence of bursts of height H in dH produced by a particle which has s in ds. The differential burst size distribution $g(H)$ is obtained by integrating the above expression over the entire range of s. If P_c is the lower limit of p/mc in a given calculation, then the limits for this integration are obtained by transforming the lines, $s=1$ and $s=1+1/P_c^2$, $l=0$, and $l=1$ into the (H,s) plane. The result is:

$$g(H,P_c)=1.1KH\int_1^{1+1/P_c^2}\frac{ds}{s^2(s-1)^{0.45}},\quad 0\leq H\leq 1,$$

and

$$g(H,P_c)=1.1KH\int_H^{1+1/P_c^2}\frac{ds}{s^2(s-1)^{0.45}},$$

$$1\leq H\leq(1+1/P_c^2). \tag{10}$$

Finally, the integral burst size distribution $G(H,P_c)$ is obtained by numerically integrating:

$$G(H,P_c)=\int_H^\infty g(H,P_c)dH. \tag{11}$$

An integral burst size distribution as so calculated is a universal one for all components of the primary beam which have integral number spectra of the form $KP^{-1.1}$ and which have the same value of P_c. To obtain a final burst size distribution—for comparison with experimental results—it is necessary to combine the distributions for the components of various Z (reverting to absolute units of H), using known or assumed absolute directional intensities for each component, the Koenig plots of fraction of the solid angle available for particles with different values P_c, and the geometrical factor of the chamber.

TABLE IV. Lowest possible values of P_c for penetration of apparatus plus residual atmosphere (1.8 g cm^{-2} for sum).

Z	P_c
6	0.40
7	0.42
8	0.44
13	0.51
19	0.57
26	0.62

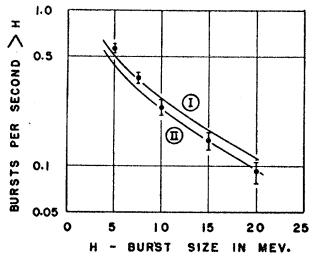

FIG. 16. Comparison of observed integral burst size distribution for Flights 21 and 22 (data combined) with the expected distribution (curve I). Observed rates are absolute; and curve I, likewise absolute, was independently calculated from emulsion data of other workers. See Sec. IV-G. Curve II is explained in Sec. V-A.

Table III, based on references 7 and 24 and Fig. 15, summarizes the basic data which were adopted as representing the known intensities and Z spectrum of heavy nuclei having P greater than the value shown. In accordance with previous discussion each component was taken to have an integral number spectrum of the form $J_Z(P)=K_ZP^{-1.1}$, where the subscript is specific to the Z of the component under consideration. It will be noted that within the C, N, O group and within the $Z\geq 10$ group a subdivision of component intensities has been made. This subdivision, though to some extent arbitrary, was based on study of the referenced Z distributions as well as others of a related nature.

In calculating families of expected burst size distributions at a given latitude, the cut-off value P_c is set by one or more of three considerations: (a) geomagnetic theory, (b) arbitrary assumption, and (c) the ionization range limit of the apparatus walls plus the residual atmosphere. In case (a) the value of P_c, in general, varies over the hemisphere of solid angle; but in any given direction its value is the same for all components with $Z\geq 2$, to within the approximation adopted herein that the ratio $Z/A=0.5$, irrespective of the atomic number Z and the atomic weight A.

The lowest possible values of P_c are determined by consideration (c) and are, of course, a function of Z. Their numerical values are listed in Table IV.

The calculations were performed in a piecewise manner appropriate to the case at hand.

V. INTERPRETATION

A. Discussion of Data from Flights 21 and 22 ($\lambda=56°$)

Flights 21 and 22 were made at $\lambda=56°$ which is about the same latitude as the most northerly point ($\lambda=55°$) at which the intensities of the heavy primaries have been measured by the photographic emulsion technique, as well as the northern limit for balloon methods because of the atmospheric depth limitation. Although emulsion observations yield only crude values of absolute intensities, they have well-established validity in the identification of tracks of heavy particles. Hence the comparison between observed ionization chamber data and those calculated from emulsion intensities provides an important measure of validation to the ionization chamber results.

In Fig. 16 is shown the observed burst size distribu-

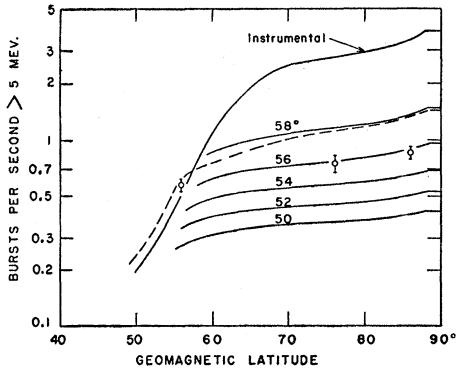

FIG. 17. Comparison of latitude dependence of observed rate of bursts greater than 5 Mev above the atmosphere with curves calculated on various assumptions. Solid curves calculated for spectra of Eqs. (12) of Sec. V-**B** of text with $P_{\min}$ assigned values equal to geomagnetic cutoff in vertical direction at geomagnetic latitudes 50°, 52°, 54°, 56°, and 58°, respectively, and finally the values given in Table IV for ionization range limit of apparatus plus residual atmosphere. The labels on curves specify the assumed spectral cutoff. Dashed curve calculated for spectra of Eqs. (16) of Sec. V-**B** of text assuming only instrumental cutoff.

tion data above the atmosphere obtained by combining the results of Flights 21 and 22. Curve I, likewise on an absolute scale, is the distribution calculated by the method of Sec. IV-**G** from the entirely independent emulsion data. The maximum difference between the calculated curve and the experimental points is for bursts greater in size than 20 Mev, and is 17 percent. The difference between the experimental and calculated values is less than twice the statistical standard deviation for each of the experimental points. Thus, there is very good agreement between the calculated and experimental distributions, especially if the uncertainties in the emulsion intensities are considered. To normalize the calculated curve to the experimental value for bursts larger than 15 Mev requires an over-all reduction of 14 percent in the K_Z's of Table III. The burst size distribution obtained by reducing all K_Z's by 14 percent is also plotted in Fig. 16 as Curve II. This curve is interesting in light of the discussion of the contribution of bursts due to stars (Sec. IV-**B**). In that discussion it was pointed out that the number of observed bursts in the size range 5 to 10 Mev was probably somewhat greater than the number due to traversals of heavy primaries, but that for bursts larger than 10 Mev, the observed bursts were produced almost entirely by heavy primaries. A comparison of the adjusted Curve II and the experimental points shows that there is complete agreement for bursts larger than 10 Mev and that the observed bursts in the size range 5 to 10 Mev are more numerous than those calculated on the assumption of a "zero wall thickness chamber." This is the result to be expected in view of the discussion of Sec. IV-**B**.

The intensity values of Table III will, however, be adhered to in spite of the indication that they are slightly too high.

Figure 16 and the associated discussion thus serve as an over-all validation of the ionization chamber technique for measuring the intensities of heavy nuclei above the atmosphere. See also reference 9. In addition, the previously expressed belief that nuclear stars are minor contributors to the burst size distribution is seen to be substantiated.

B. Interpretation of Data from Flights at Higher Latitudes

Interpretation of the observed burst size distributions of Flight 15 at $\lambda=76°$ and of Flight 17 at $\lambda=86°$ can now proceed with confidence.

For this purpose families of burst size distributions were calculated on the assumption that the integral number spectra of all heavy components of the primary radiation continued to have the form (4) down to some value $P_{\min}$ and that they were flat at lower values of P. That is, it was assumed that:

$$\begin{aligned} J_Z(P) &= K_Z P^{-1.1}, \quad && P \geq P_{\min}, \\ &= K_Z P_{\min}{}^{-1.1}, && P \leq P_{\min}, \end{aligned} \tag{12}$$

for all $Z \geq 6$, with values of K_Z given in Table III.

$P_{\min}$ was assigned values equal to the geomagnetic cutoffs in the vertical direction at geomagnetic latitudes 50°, 52°, 54°, 56°, and 58° and finally the values given in Table IV for the ionization range limit of the apparatus plus residual atmosphere.

Figures 17, 18, and 19 show the experimental points at latitudes 56°, 76°, and 86° for the counting rate of bursts larger than 5, 10, and 20 Mev, respectively. And they show families of smooth curves calculated for various values of $P_{\min}$ listed above. The uppermost curve in each of the figures is the one limited only by geomagnetic considerations and eventually at the more northerly latitudes by the ionization range of the apparatus. The continued rise of each of the curves north of the latitude equal to the labeled latitude of

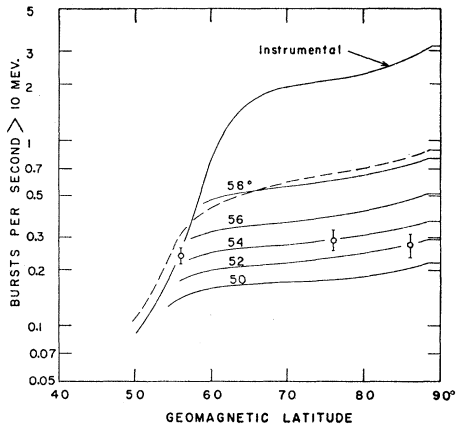

FIG. 18. Same as Fig. 17 except for rate of bursts greater than 10 Mev.

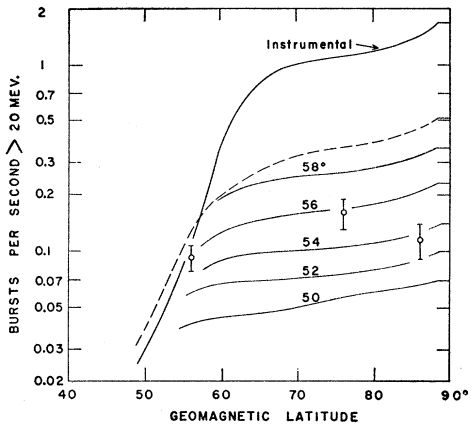

FIG. 19. Same as Fig. 17 except for rate of bursts greater than 20 Mev.

assumed cutoff ($P_{\min}$) is due to the progressive opening up of the earth's shadow cone as one goes to higher latitudes.[21–23] The values used for $P_{\min}$ in the vertical direction at various latitudes are listed in Table V. It is evident that the observed results are altogether inconsistent with the absence of a cutoff in the spectrum. Thus at 76° and at 86° the expected counting rates on the assumption of no cutoff (other than the instrumental one) are about four times as great as the observed ones for bursts larger than 5 Mev, about eight times as great as for bursts larger than 10 Mev, and about ten times as great as for bursts larger than 20 Mev.

The observed data are, however, clearly consistent with the spectral form (12) in which there is a *general spectral cutoff* at

$$P_{\min}\equiv(p/mc)_{\min}\approx 0.8. \tag{13}$$

The corresponding value of magnetic rigidity is

$$R_{\min}\approx 1.54\times 10^9 \text{ volts}. \tag{14}$$

The spectral range between the value of $P_{\min}$ quoted in Eq. (13) and the instrumental limits listed in Table IV is rather small. It is therefore appropriate to note the reason for the large ratio between the apparatus cutoff curves in Figs. 17, 18, and 19 and those corresponding to a general cutoff at $P_{\min}=0.8$. Since the ionization chamber is already detecting particles of $Z\geq 10$ with rather high efficiency the contribution of such particles in the range ~ 0.8 to ~ 0.55 is not a major one. However, there is a great increase in efficiency in detection of C, N, O nuclei in the range ~ 0.8 to ~ 0.42. For example, the specific ionization corresponding to $P=0.68$ is 3.2 times minimum and only about 27 percent of C, N, O nuclei give bursts larger than 5 Mev and a negligible fraction give bursts larger than 10 Mev. But just above the instrumental cutoff, about 76 percent of C, N, O nuclei yield bursts greater than 5 Mev, about 57 percent greater than 10 Mev and about 47 percent greater than 20 Mev. Hence the comparisons exhibited in Figs. 17, 18, and 19 and discussed above refer most significantly to the C, N, O group. Their significance for nuclei having $Z\geq 10$ is not as strong.

The whole body of data appears to the present authors to be most naturally consistent with a complete absence of primary heavy nuclei having magnetic rigidities less than about 1.54×10^9 volts.

It is nonetheless of interest to consider other possibilities. The Rochester group[7] has proposed an integral number spectrum for heavy nuclei of the form:

$$J(\epsilon)=K/(1+\epsilon)^{1.35}, \tag{15}$$

where ϵ is the kinetic energy per nucleon.

Recently Ney[25] has reviewed all available emulsion intensity data from balloon flights and has proposed the integral number spectra:

$$J_{C,N,O}(\epsilon)=[0.0020/(1+\epsilon)^{1.25}]\ \text{cm}^{-2}\ \text{sec}^{-1}\ \text{sterad}^{-1},$$

and (16)

$$J_{Z\geq 10}(\epsilon)=0.0010/(1+\epsilon)^{1.5}.$$

The dashed curves in Figs. 17, 18, and 19 represent the expected counting rates in the chambers of the present investigation for the spectra (16). The calculated curves are clearly inconsistent with the experimental points at high latitudes.

VI. SIGNIFICANCE OF RESULTS

A. General Comments

(a) Throughout this paper explicit faith has been placed in the common belief that the "latitude effects" in cosmic-ray studies are to be attributed to a geomagnetic field conveniently described as that due to a point dipole of magnetic moment $M=8.1\times 10^{25}$ gauss cm^3, located near the geometrical center of the solid earth. Some doubt in this belief has recently been expressed. But no significant modification has been offered; and it appears that the reasons for the doubt are much less convincing than the reasons for belief in a simple dipole field.

It is well known[26] that a full harmonic analysis of the observations of the surface magnetic field of the earth yields a more complex description of the geomagnetic field. The only feature of the more complex description

TABLE V. Geomagnetic cut-off values of P in the vertical direction at various latitudes.

λ	$P_{\min}$
50°	1.32
52°	1.10
54°	0.91
56°	0.75
58°	0.61

[25] E. P. Ney, Duke University, Cosmic Ray Conference of the National Science Foundation, November 30, December 1, 2, 1953 (unpublished).

[26] S. Chapman and J. Bartels, *Geomagnetism* (Oxford University Press, London, 1940), Vol. 2.

which appears to be significant in cosmic-ray effects is the slight displacement from the center of the earth of the "best dipole." This eccentric-dipole representation has been invoked by a number of writers in interpreting "longitude effects" and in making corrections to geomagnetic latitudes and to distances from the dipole to the point of observation. In the present work the centered-dipole representation has been employed, though it is realized that slight numerical corrections may eventually be worthwhile.

(b) Measurements above the atmosphere on the intensities of heavy nuclei are reasonably presumed to be free of albedo effects: i.e., of the effects of secondaries emerging from, and in some cases returning to, the atmosphere. In this sense their interpretation is notably simpler than the interpretation of total intensity measurements.[5] But due to the low intensity of the heavy nuclei it is more difficult to obtain precise results.

B. Conclusions

(a) The present paper apparently contains the only available information on the low-momentum end of the spectra of heavy primary cosmic rays. Although the accuracy of the data is not as high as would be desired, it appears that it will be difficult to substantially improve it.

(b) The data demonstrate a complete or nearly complete absence of primary heavy nuclei of $Z=6$, 7, and 8 having magnetic rigidities in the range 1.5×10^9 to 0.8×10^9 volts. As previously remarked, the observations are most naturally understood in terms of a complete absence. But the accuracy of the data is not such as to positively exclude an intensity in the above rigidity range of as much as 15 percent of the integral intensity for $R>1.5\times10^9$ volts.

(c) The present results are not as restrictive for nuclei having $Z\geq10$ but are again most naturally consistent with a complete spectral absence in the rigidity range 1.5×10^9 to about 1.1×10^9 volts. However, an increase of integral intensity of 30 percent between 1.5×10^9 and 1.1×10^9 is not positively excluded.

(d) The results are clearly inconsistent with the spectra of Eq. (16).

(e) Any contribution to the observed counting rates by primary Li, Be, or B nuclei must be by ones of magnetic rigidity considerably less than the general spectral cutoff at $R\sim1.5\times10^9$ volts. For this reason and for the further reason that the increase in counting rates with latitude is already completely accounted for by nuclei of $Z\geq6$ and of $R>1.5\times10^9$ volts, no further consideration has been given to Li, Be, and B.

(f) Special significance may be attributed to the fact that the cutoff in the spectra of the heavy nuclei occurs at very closely the same value of *magnetic rigidity* as the cutoff in the spectrum of primary protons,[1–5] and *not* at the same value of *velocity*. Thus, since $Z/A=1$ for a proton and ~0.5 for all heavier nuclei, pairs of "latitude knees" for the same cut-off velocity would be as follows: 58° for protons, 51° for heavies; 56°, 48°; 54°, 46°; and 52°, 43°. The existence of any such corresponding latitude knees is believed to be excluded beyond any reasonable question. Hence, it is strongly suggested that the physical mechanism responsible for the cutoff in the spectra of both protons and heavy nuclei is one of *magnetic character* and not, for example, one of ionization range in material, interstellar or otherwise. Such a conclusion would seem to support the classical hypothesis of Janossy, Epstein, and Vallarta that a heliomagnetic field deflects charged particles of low magnetic rigidity and of non-solar-system-origin away from the vicinity of the earth's orbit. But such an hypothesis has recently fallen into disfavor for a number of reasons:[27]

(i) The model of the sun and the earth—each with its simple dipole magnetic moment, imbedded in a complete vacuum—is a significantly inadequate representation of present astrophysical knowledge.

(ii) The direct spectral observations of magnetic fields in the sun's atmosphere by Babcock, by Thiessen, and by von Kluber, though difficult and of limited accuracy, definitely exclude a general dipole moment as large as 0.6×10^{34} gauss cm^3—as would be needed to account for the cosmic ray cutoff.

(iii) The observed diurnal variation in total cosmic ray intensity at balloon altitudes is an order of magnitude smaller than that expected to be produced by such a solar magnetic dipole.[28]

(g) No promising alternative explanation of the cutoff in the spectra of primary cosmic rays is known to the present authors. But it now appears necessary that the explanation be of magnetic character.

VII. ACKNOWLEDGMENTS

The authors are particularly indebted to Lt. Malcolm S. Jones, Jr., U. S. N., formerly of the Nuclear Physics Branch of the Office of Naval Research, for able and enthusiastic support of all phases of this work, for personally leading the firing expedition, and for the resourceful development of a satisfactory rocket igniter under primitive shipboard conditions. Flights 8, 15, and 17 were launched from the U. S. Navy icebreaker—U. S. S. Staten Island—and Flights 21 and 22 from the U. S. Coast Guard icebreaker—U. S. C. G. C. Eastwind—with the cooperation and essential assistance of the officers and men of these vessels. The rocket propulsion units, known by the code name "Deacon," were manufactured by the Allegany Ballistics Laboratory of Cumberland, Maryland, and provided by the Navy Bureau of Aeronautics. The balloons were plastic ones

[27] The authors are particularly indebted to Professor Spitzer, Professor Schwarzschild, and Professor Gold for illuminating discussions of this matter.

[28] Firor, Jory, and Treiman, Phys. Rev. **93**, 551 (1954).

of the General Mills Company of Minneapolis. Launching of the rockoons was supervised by engineers of the General Mills Aeronautical Laboratories. Firing circuits were made at the Naval Research Laboratory through a cooperative arrangement with Herman La Gow and Carl Medrow. The special nose shells were fabricated by Weber Brothers Metal Works of Chicago. The scientific apparatus, including telemeters, was designed and built at the State University of Iowa. Aerodynamic and mechanical design of the rocket fins and of the nose assemblies was also performed there and the components were built in the shops of the Department of Physics under the able supervision of J. G. Sentinella. Important experimental assistance was given by L. H. Meredith and Lee F. Blodgett of the Cosmic Ray Laboratory.

PHYSICAL REVIEW VOLUME 95, NUMBER 1 JULY 1, 1954

Cloud-Chamber Study of Charged V Particles*

CARL M. YORK, JR., R. B. LEIGHTON, AND E. K. BJØRNERUD
California Institute of Technology, Pasadena, California

(Received March 31, 1954)

An analysis of 103 charged V-particle decays is presented. These events have been observed with a double cloud chamber operated at 1750-m altitude. The events in the upper chamber appear to have markedly different properties from those in the lower. The particles in the upper chamber have measured properties which are in every respect consistent with those of the κ meson. Their lifetime is in the range 5×10^{-10} to 2×10^{-8} sec; their mass is $\sim1000\ m_e$; their transverse momentum distribution is consistent with a three-body decay scheme; the momentum in the center-of-mass system of their charged decay products is also consistent with three-body decay; and their frequency of production is greater than 0.4 percent of the total number of shower particles observed. On the other hand, the particles observed in the lower chamber have a lifetime in the range 10^{-11} to 3×10^{-10} sec; their transverse momentum distribution is consistent with a two-body decay scheme; their frequency of production is greater than 0.8 percent of the total number of shower particles; they are observed with approximately one-third of the frequency of Λ^0 particles; and they apparently can be produced in meson-nucleon collisions. The majority of the particles in the lower chamber are tentatively identified as charged hyperons with the aid of two cases which appear to have proton secondaries. The proposed decay scheme is $V_1^+\rightarrow p+\pi^0+Q$; and in order to fit all of the data, the alternate mode of decay, $V_1^+\rightarrow\pi^++n+Q$ must be introduced. The Q value is estimated to be $\lesssim125$ Mev.

I. INTRODUCTION

SINCE the original observation by Rochester and Butler[1] of the decay of a charged particle of mass greater than $900m_e$ into a light meson, extensive investigation of the decay of heavy charged particles has been carried out. The evidence has come from three distinct experimental sources, *viz.* cloud chambers in magnetic fields,[2–6] photographic emulsions,[7–10] and multiplate cloud chambers,[11] and has been interpreted in terms of a number of different particles:

(a) The majority of these observations can be explained in terms of a single particle (called a κ meson) of mass about $1000m_e$, which decays into a single, light, charged meson and two or more neutral particles. There is direct evidence that this charged meson is a μ meson from its characteristic decay into an electron.[7]

(b) There are also some data suggesting the existence of a different particle, the so-called χ meson,[8] of mass about $1000m_e$ which decays into a charged π meson and one neutral particle. The evidence relating to the χ meson is not very firm at present, but this decay scheme has been considered as a possibility in interpreting the present data.

(c) There is conclusive evidence for the existence of τ mesons ($m\approx965m_e$) which decay into three π mesons.[9]

(d) Recently, evidence has been presented which indicates that there may be a positively charged V particle of greater than nucleonic mass which decays into a nucleon and meson.[8–10,12]

(e) Finally, there are rather convincing indications of the existence of a "cascade" decay of a still heavier,

* Assisted in part by the joint program of the U. S. Office of Naval Research and the U. S. Atomic Energy Commission.

[1] G. D. Rochester and C. C. Butler, Nature **160**, 855 (1947).
[2] Seriff, Leighton, Hsiao, Cowan, and Anderson, Phys. Rev. **78**, 290 (1950).
[3] R. B. Leighton and S. D. Wanlass, Phys. Rev. **86**, 426 (1952).
[4] Armenteros, Barker, Butler, Cachon, and York, Phil. Mag. **43**, 597 (1952).
[5] Astbury, Chippindale, Millar, Newth, Page, Rytz, and Sahiar, Phil. Mag. **43**, 1283 (1952).
[6] Astbury, Chippindale, Millar, Newth, Page, Rytz, and Sahiar, Phil. Mag. **44**, 242 (1953).
[7] C. O'Ceallaigh, Phil. Mag. **42**, 1932 (1951).
[8] Report of the Bagneres Conference, 1953 (unpublished).
[9] Lal, Pal, and Peters, Phys. Rev. **92**, 438 (1953).
[10] Bonetti, Levi-Setti, Panetti, and Tomasini, Nuovo cimento **10**, 1729 (1953).
[11] Bridge, Courant, DeStaebler, and Rossi, Phys. Rev. **91**, 1024 (1953). (This reference contains a complete bibliography of the earlier work of this group.)
[12] York, Leighton, and Bjørnerud, Phys. Rev. **90**, 167 (1953).